SUPPLEMENTARY INFORMATION APPENDIX

Positive allosteric modulation of indoleamine 2,3-dioxygenase 1 restrains neuroinflammation

Giada Mondanelli, Alice Coletti, Francesco Greco, Maria Teresa Pallotta, Ciriana Orabona, Alberta Iacono, Maria Laura Belladonna, Elisa Albini, Eleonora Panfili, Francesca Fallarino, Marco Gargaro, Giorgia Manni, Davide Matino, Agostinho Carvalho, Cristina Cunha, Massimiliano Di Filippo, Lorenzo Gaetani, Roberta Bianchi, Carmine Vacca, Ioana Maria Iamandii, Elisa Proietti, Francesca Boscia, Lucio Annunziato, Maikel Peppelenbosch, Paolo Puccetti, Paolo Calabresi, Antonio Macchiarulo, Laura Santambrogio, Claudia Volpi, and Ursula Grohmann

Ursula Grohmann, Ph.D. (ursula.grohmann@unipg.it)

Claudia Volpi, Ph.D. (claudia.volpi@unipg.it)

University of Perugia
Department of Experimental Medicine
Piazzale Gambuli, n. 1 (C Bldg, 4th Fl)
Perugia 06132, Italy

This Supplementary File includes:

Supplementary Figures 1 to 6 with Legends
Supplementary Tables 1 to 6
Materials and Methods with references

www.pnas.org/cgi/doi/10.1073/pnas.1918215117

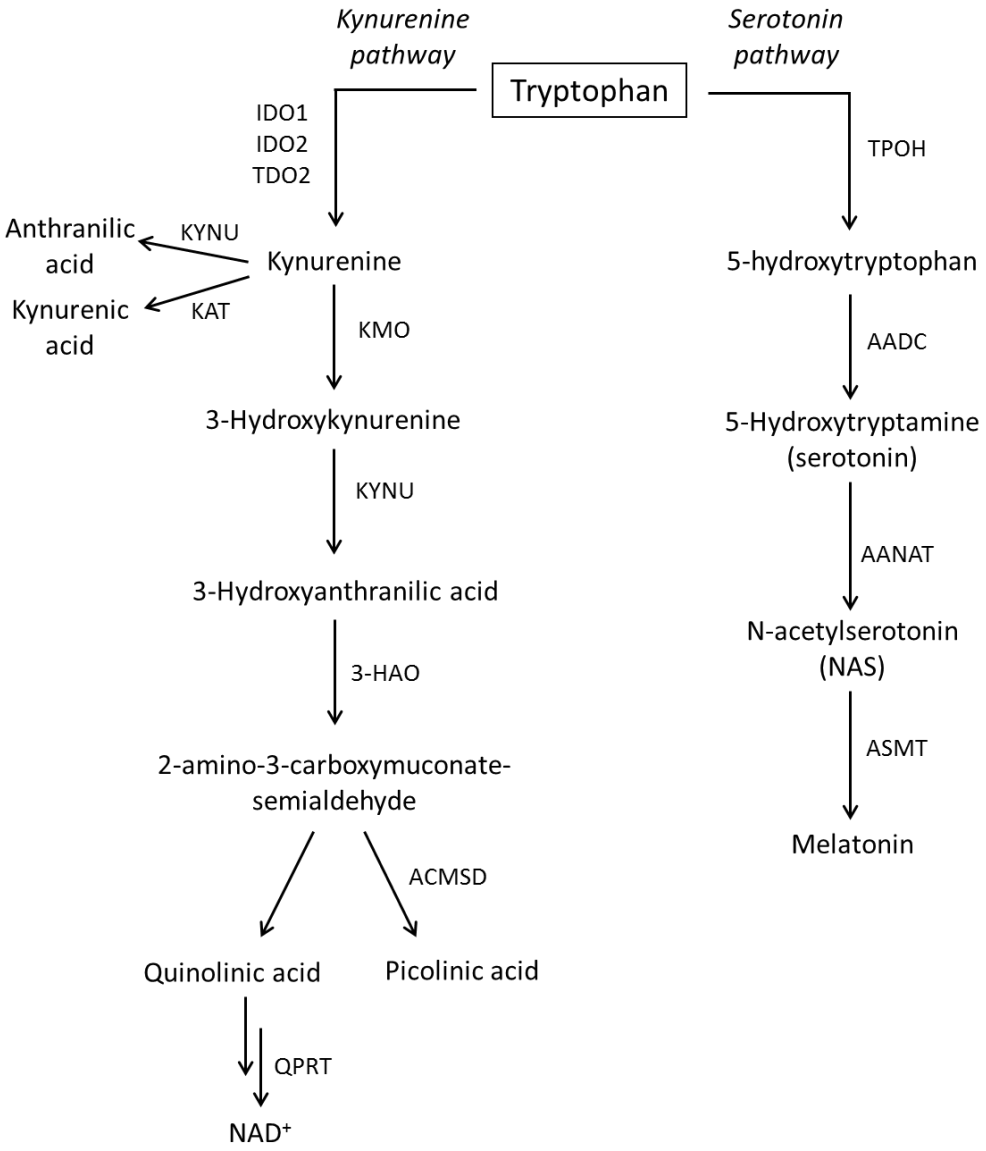

Fig. S1. Trp metabolism along the kynurenine and serotonin pathways. Abbreviations: AADC, aromatic L-amino acid decarboxylase; AANAT, alkylamine N-acetyltransferase; ACMSD, aminocarboxymuconate semialdehyde decarboxylase; ASMT, acetylserotonin O-methyltransferase; 3-HAO, 3-hydroxyamino oxidase; IDO1 and IDO2, indoleamine 2,3-dioxygenases 1 and 2; KAT, kynurenine aminotransferase; KYNU, Kynureninase; KMO, kynurenine 3-monooxygenase; QPRT, quinolinate phosphoribosyltransferase; TDO, tryptophan 2,3-dioxygenase, TPOH, tryptophan-5-hydroxylase.

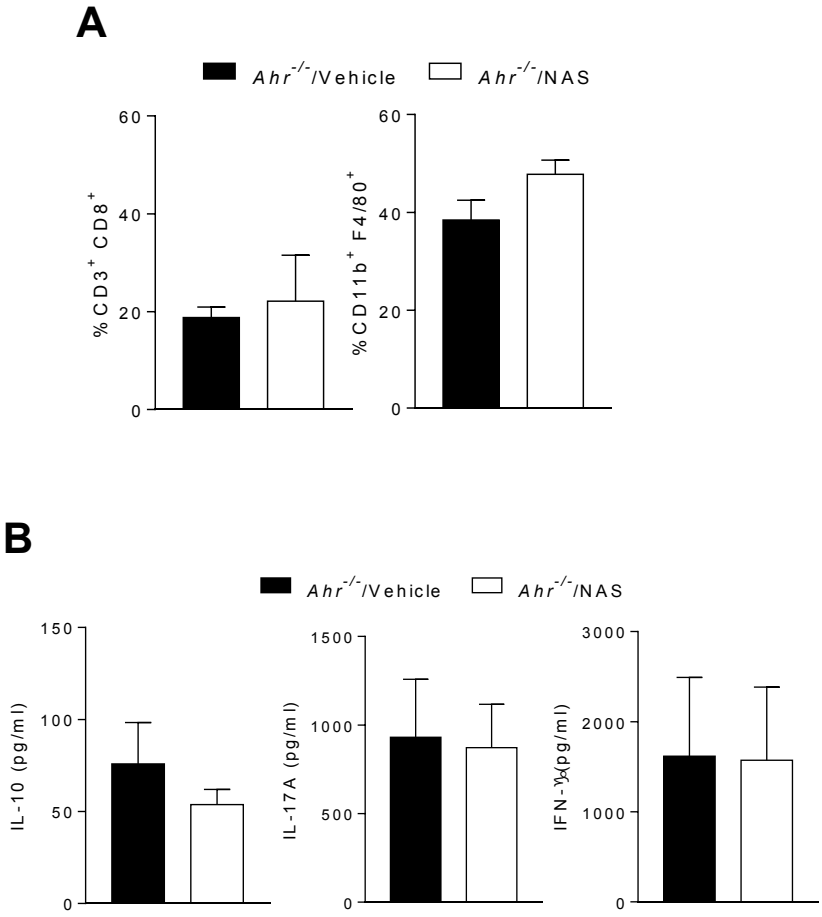

Fig. S2. AhR expression is required for NAS protective effects in EAE. (*A*) Percentages of $CD3^+CD8^+$ and $CD11b^+F4/80^+$ cells in the spinal cord of $Ahr^{-/-}$ mice, treated with NAS (10 mg/kg) or vehicle alone every other day until 24 d, at 25 d after immunization with the MOG peptide. (*B*) Cytokine production by $CD4^+$ T cells sorted at 25 d after immunization with the MOG peptide from cervical lymph nodes from mice with EAE and restimulated with MOG or medium alone *in vitro* for 24 h. Data (analyzed in triplicates) are from two experiments.

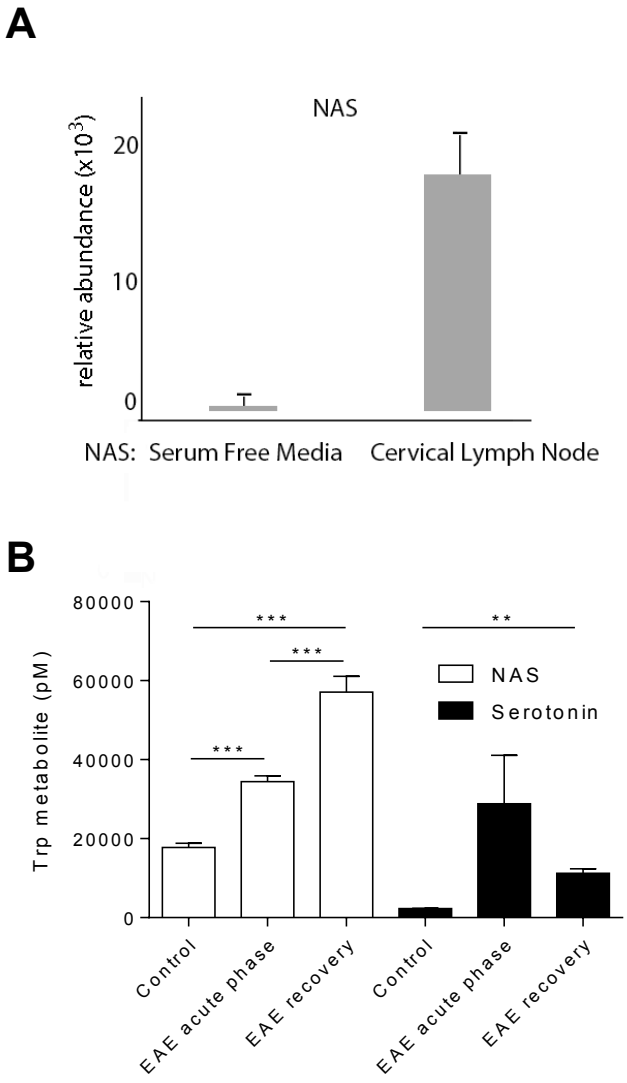

Fig. S3. High levels of NAS are present in cervical lymph nodes of mice with EAE in the recovery phase. **(***A***)** Metabolomic analysis of NAS contents in cervical lymph nodes of healthy C57/BL6 mice as compared to serum-free media was performed by mass spectrometry. (*B*) NAS and serotonin contents in cervical lymph nodes in C57/BL6 mice at different times after MOG sensitization. Control, day 0. EAE acute phase, day +14. EAE recovery phase, day +28.

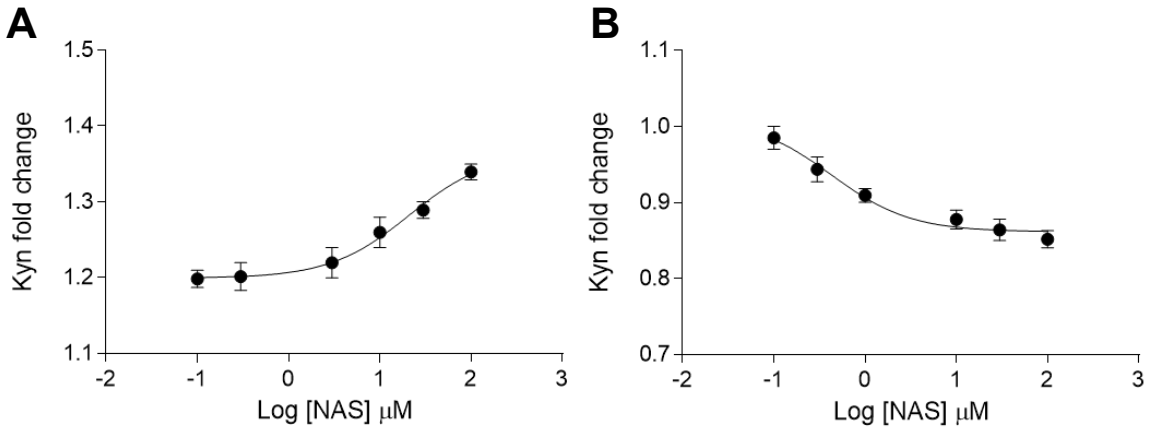

Fig. S4. NAS exerts enhancing catalytic effects on human IDO1 but not mouse TDO. (*A*) Effect of NAS at different concentrations on Kyn release in 24 h by P1.HTR cells transfected with human WT IDO1. (*B*) Effect of NAS at different concentrations as in (*A*) on Kyn release in 24 h by P1.HTR cells transfected with mouse TDO. Trp was used at 10 μM. Results are the mean±SD. of the Kyn fold change (relative to the buffer without Trp metabolites) of three independent experiments, each performed in triplicate. Control absolute values of Kyn (medium without NAS) were 8.2 μM ± 1.1 (*A*) and 14.93 μM ± 5.3 (*B*).

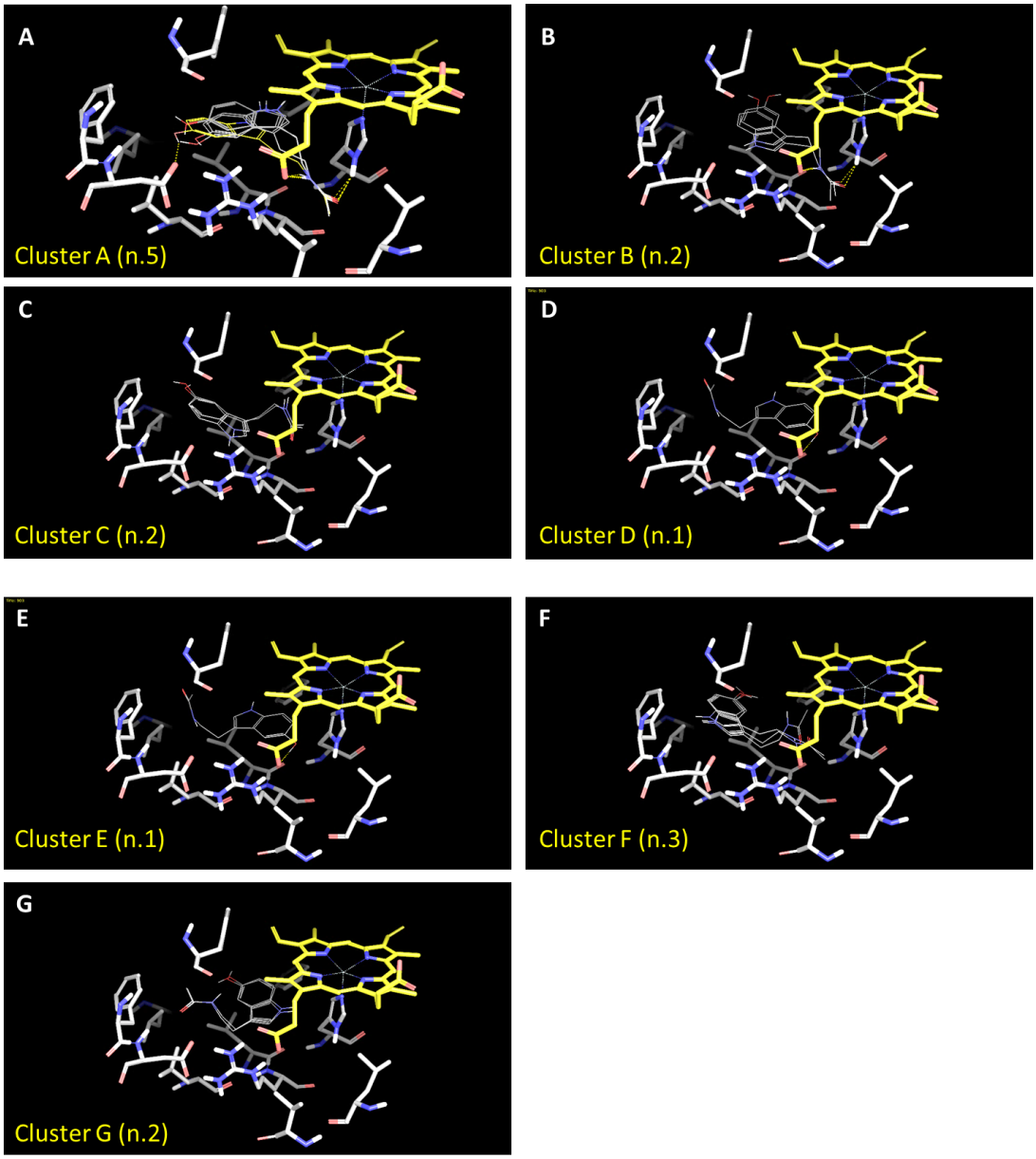

Fig. S5. Possible binding modes of NAS into the allosteric pocket of IDO1. Energy scored solutions are depicted for each cluster (*A*-*G*; Table S2) with ligand and protein being colored by atom types (heme group is shown with yellow carbon; NAS and protein are shown with gray carbon).

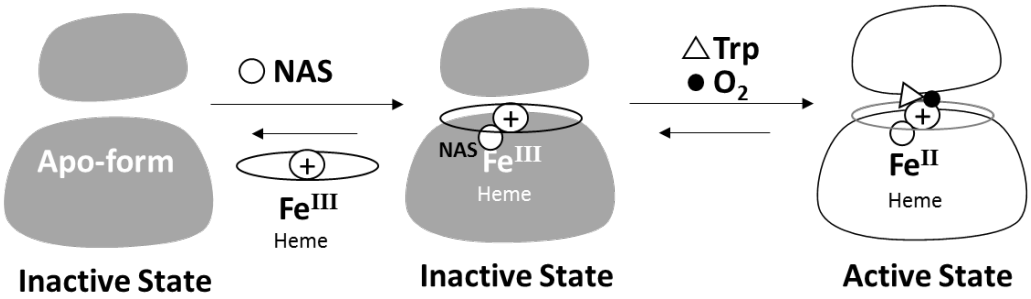

Fig. S6. Scheme of the possible model of NAS modulation of IDO1 activity. NAS binds to the allosteric pocket of IDO1 and promotes an equilibrium shift towards the heme-bound form of the enzyme that will become catalytically active upon redox reaction of the heme cofactor.

Table S1. EAE in WT and *Ido1*$^{-/-}$ mice.

Mice	Treatment	(*n*)	Incidence (%)	Mortality (%)	Day of onset (mean ± SD)	Maximum score (mean ± SD)
WT	vehicle	21	100	0	12.8 ± 1.6	2.8 ± 0.33
WT	NAS	21	84	0	16.0 ± 1.6[a]	1.7 ± 0.42[c]
Ido1 $^{-/-}$	vehicle	21	95	0	11.3 ± 1.5	2.5 ± 0.45
Ido1 $^{-/-}$	NAS	21	96	0	12.5 ± 1.1[b]	2.7 ± 0.32[d]

[a], $P = 0.018$ (NAS *versus* vehicle in WT mice)
[b], $P = 0.070$ (NAS *versus* vehicle in *Ido1*$^{-/-}$ mice)
[c], $P = 0.005$ (NAS *versus* vehicle in WT mice)
[d], $P = 0.100$ (NAS *versus* vehicle in *Ido1*$^{-/-}$ mice)

Table S2. Top scored binding poses of NAS into the allosteric pocket of IDO1 and clustering analysis.

POSE	Docking Score	Glide Score (kcal/mol)	Cluster
#1	-7.91	-7.91	A
#2	-7.59	-7.59	A
#3	-7.59	-7.59	A
#4	-7.59	-7.59	A
#5	-7.55	-7.55	B
#6	-7.52	-7.52	B
#7	-7.02	-7.02	A
#8	-6.84	-6.84	C
#9	-6.62	-6.62	C
#10	-6.40	-6.40	D
#11	-6.29	-6.29	E
#12	-6.11	-6.11	F
#13	-5.96	-5.96	G
#14	-5.90	-5.90	F
#15	-5.90	-5.90	G
#16	-5.81	-5.81	F

Table S3. Characteristics of patients with RRMS and control subjects recruited in the study.

	RRMS	Controls
Number	59	32
Females/males	42/17	20/12
Mean age (years)	41.01 ± 10.19[a]	40.24 ± 9.12
Mean age of onset (years)	32.44 ± 10.77	ND
Mean duration of MS (years)	8.20 ± 5.86	ND
EDSS score	1.58 ± 1.53	ND
Ongoing treatment		
Dimethyl fumarate	16 (27.1)[b]	0
Natalizumab	16 (27.1)	0
Glatiramer acetate	8 (13.5)	0
Interferons	7 (11.8)	0
Fingolimod	3 (5.0)	0
Alemtuzumab	1 (1.7)	0
Ocrelizumab	1 (1.7)	0
None	7 (11.8)	32 (100)

[a] Data are shown as the mean ± SD.

[b] Number of patients treated with the specific drug (percentage over total number of patients)

ND, not determinable

EDSS, Expanded Disability Status Scale

Table S4. Description of haplotype-tagging SNPs in the *IDO1* gene.

RefSNP	Genome coordinates	Genomic location	Alleles	CEU MAF	HWE
rs9657182	chr8:39908329	Near gene 5’	T>C	0.483	0.64
rs3808606	chr8:39911856	Near gene 5’	C>T	0.481	0.29
rs10089078	chr8:39912420	Near gene 5’	G>A	0.336	0.52
rs7820268	chr8:39920010	Intron	C>T	0.305	0.99
rs3739319	chr8:39927802	Intron	G>A	0.429	0.78

SNP, single nucleotide polymorphism; CEU, Utah Residents (CEPH) with Northern and Western Ancestry; MAF, minor allele frequency; HWE, Hardy-Weinberg equilibrium. Genome coordinates were extracted from the GRCh38.p12 build.

Table S5. Allele distributions of single nucleotide polymorphisms (SNPs) in the *IDO1* gene among patients with MS and healthy controls, and association test results.

SNP rs# number	Alleles[a]	Minor allele frequencies (%)		*P* value[b]
		T1D	Controls	
rs9657182	T>C	0.429	0.427	0.853
rs3808606	C>T	0.453	0.457	0.748
rs10089078	G>A	0.383	0.368	0.421
rs7820268	C>T	0.323	0.417	**0.007**
rs3739319	G>A	0.446	0.477	0.227

[a] The major and minor alleles are represented by the first and second nucleotides, respectively.

[b] *P* values were calculated using the Haploview 4.2 software. Significant associations are reported in bold.

Table S6. Primer sequences used in the study.

Gene		Primer sequence
Ido1	F	5-CGATGTTCGAAAGGTGCTGC-3′
	R	5-GCAGGAGAAGCTGCGATTTC-3′
Cyp1a1	F	GACACAGTGATTGGCAGAG
	R	GAAGGTCTCCAGAATGAAGG
Gapdh	F	5-CTGCCCAGAACATCATCCCT-3′
	R	5-ACTTGGCAGGTTTCTCCAGG-3
IDO1	F	5’-TCACAGACCACAAGTCACAG-3′
	R	5’-GCAAGACCTTACGGACATCT-3′
ACTB	F	5’-TCAGGGTGAGGATGCCTCTC-3′
	R	5’-CTCGTCGTCGACAACGGCT-3′

F, forward; R, reverse.

Materials and Methods

Mice and Cell Lines. Eight- to ten-week-old female C57BL/6 mice were obtained from Charles River Breeding Laboratories. IDO1-deficient mice (*Ido1*$^{-/-}$) were purchased from The Jackson Laboratory and bred at Charles River Breeding Laboratories. B6.129-Ahrtm1Bra/J mice deficient for AhR (*Ahr*$^{-/-}$) were bred at the animal facility of the University of Perugia, according to the University of Perugia Animal Care and Use Committee guidelines (Italian Approved Animal Welfare Assurance A-3143-01). The *in vivo* experiments performed in this work were approved by the Italian Ministry of Health. All knockout mice used in these studies were genotyped by PCR of DNA isolated from tail clippings. P1.HTR (P1), a highly transfectable clonal variant of mouse mastocytoma P815, was cultured in Iscove's modified Dulbecco's medium supplemented with 10% FCS at 37°C.

Transfection of P1.HTR cells. Constructs expressing mouse *Ido1* and human *IDO1* were generated from the cDNA of mouse conventional dendritic cells (cDCs), as previously described (1, 2), and peripheral blood mononuclear cells (PBMCs), both stimulated with IFN-γ, respectively. The construct expressing mouse *Tdo2* was generated from mouse liver. Twenty μg DNA was used to transfect 1×10^7 P1.HTR cells by electroporation and stable transfectants were obtained by puromycin selection. P1.HTR cells, stably transfected with the empty plasmid, were used as control.

Subject Recruitment and Purification of Peripheral Blood Mononuclear Cells (PBMCs). Peripheral venous blood (5 ml) was obtained from patients with relapsing-remitting multiple sclerosis (RRMS) and age matched controls, i.e., without MS or any autoimmune or inflammatory disease, attending the Day Service of the Neurologic Clinic of S. Maria della Misericordia Hospital, Perugia, Italy during usual biological monitoring over years 2017-2019. A total of 59 patients with RRMS and 32 control subjects were recruited to this study. Typically, blood was analyzed along

side that of control subjects taken at the same time of day to avoid any potential confounding effects of diurnal rhythm and season as well as experimental variability. To limit the effects of diet on circulating L-tryptophan (Trp), serum samples were collected after an overnight fasting. Individuals included in our studies were free of known infection at the time of blood draw. Main subject demographic and disease characteristics are summarized in Table S1. The study was approved by the Ethics Committee of Health Agencies of Umbria (Ref. # 2925/16 of December 12th, 2016), and all subjects provided informed written consent for the collection of samples and subsequent analysis. PBMCs were isolated on a Ficoll-Hypaque gradient and left untreated or exposed for 24 h at 37 °C to IFN-γ (at 500 U/ml; Novus Biologicals LLC) in the presence or absence of 30 μM NAS (Sigma-Aldrich) in complete medium (RPMI with 10% FCS, 10 mM HEPES, and 50 μM 2-mercaptoethanol).

EAE induction and treatment with NAS *in vivo*. EAE was induced as described (3) in twelve-week-old wild-type (WT), *Ido1*$^{-/-}$, and *Ahr*$^{-/-}$ mice by s.c. immunization with 300 μg of the murine myelinoligodendrocyte glycoprotein (MOG) peptide 35-55 (MEVGWYRSPFSRVVHLYRNGK) emulsified in complete Freund's adjuvant. Two hundreds ng of pertussis toxin in 200 μl of phosphate-buffered saline (PBS) were injected i.p. on the day of immunization (day 0) and two days later (3-5). Neurologic signs (ascending paralysis from the tail to the forelimbs) were scored over a period of 25 days. N-acetyl serotonin (NAS; 10 mg per kg body weight) was administered i.p. every other day starting 1 d after MOG immunization for 24 d. Control mice received vehicle (PBS) alone. Mice were monitored daily, and neurological effects were scored as follows: 0, no signs of disease; 1, flaccid tail; 2, inability to right; 3, paralysis of one hind limb; 4, paralysis of both hind limbs; and 5, moribund or death.

Histology. At day 25 after MOG immunization, mice were anesthetized by i.p administration of Avertin (125 mg/kg) and perfused transcardially with 4% paraformaldehyde in PBS. Spinal cords

were removed, fixed for 24h in zinc formalin (Sigma, Z2902) and then processed and embedded in paraffin using standard procedures. Sections were cut at 5 μm and stained by Luxol fast blue stain to reveal inflammatory infiltrates in the central nervous system and to analyze the degree of demyelination.

Leukocyte Purification. Purification of spinal cord-infiltrating leukocytes was performed as described (3, 6, 7). Briefly, spinal cords were recovered from anesthetized mice perfused with cold PBS. After centrifugation of spinal cord homogenates, infiltrating leukocytes were separated on a discontinous percoll gradient (Sigma). $CD4^+$ T cells were purified from cervical lymph nodes using CD4 MicroBeads (Miltenyi Biotec). Splenic conventional DCs (cDCs) were purified by magnetic-activated cell sorting using CD11c MicroBeads and MidiMacs (Miltenyi Biotec), in the presence of EDTA to disrupt DC-T cell complexes, as described (3, 8, 9). Cells were 90-95% $CD11c^+$, >95% MHC $I\text{-}A^+$, >95% $B7\text{-}2^+$, <0.1% $CD3^+$, and appeared to consist of 90–95% $CD8^-$, 5–10% $CD8^+$, and 1–5% $B220^+PDCA^+$ cells (8, 9). For the purification of $CD8^-$ DCs, $CD11c^+$ cells were further fractionated using CD8 MicroBeads (Miltenyi Biotec). Cytokine production was measured in supernatants from cervical lymph nodes of mice at 25 d after MOG immunization, restimulated *in vitro* with the MOG peptide at 10 μM for 24 h, and cDCs incubated with different concentrations of NAS for 24 h. For Real-time PCR analysis of *Ido1* transcripts, cDCs were incubated with 30 μM NAS for 3 or 18 h. For *in vitro* studies, cDCs were cultured at 1×10^6 cells per well in 24-well plates in Iscove's Modified Dulbecco's medium (IMDM; Thermo Fisher Scientific). Peripheral blood mononuclear cells (PBMCs) were isolated on a Ficoll-Hypaque gradient and left untreated or exposed for 24 h at 37 °C to IFN-γ (500 U/ml; Novus Biologicals LLC,) in the presence or absence of 30 μM NAS in complete medium (RPMI with 10% FCS, 10 mM HEPES, and 50 μM 2-mercaptoethanol).

Flow Cytometry and Cytokine Determination. Flow cytometric analysis was performed as described (3). Briefly, cells were treated with rat anti-CD16/32 (2.4G2) for 30 min at 4 °C for the blockade of Fc receptors before assaying on an LSR Fortessa (BD Biosciences, CA, USA) flow cytometer, using FlowJo analysis software (Tree Star, OR, USA). Phenotypic characterization of immune cells was performed by extracellular staining using the following Abs: APC-CD3 (145-2C11; Biolegend, CA, USA), BV510-CD4 (RM4-5; BD Horizon, CA, USA), FITC-CD8 (Miltenyi), Percp-CD45.2 (104; Biolegend, CA, USA), PEDazzle 594-MHC II (M5/114.15.2; Biolegend, CA, USA), APC-eFluor780-CD11c (N418; Invitrogen, USA), AF700-CD11b (M1/70; Biolegend, CA, USA), BV711-F4/80 (T45.2342; BD Horizon, CA, USA). Mouse cytokines (IL-10, IL-17A, and IFN-γ) were measured in culture supernatants by ELISA using specific kits (eBioscience).

Skin Test Assay. A skin test assay was used for measurements of major histocompatibility complex class I–restricted delayed-type hypersensitivity (DTH) responses to the HY peptide (WMHHNMDLI) in C57BL/6 female recipient mice, as described (2, 9). For *in vivo* immunization, 3×10^5 peptide-loaded $CD8^-$ DCs, combined with a minority fraction (5%) of peptide-loaded WT, *Ido1*$^{-/-}$, or *Ahr*$^{-/-}$ $CD8^-$ DCs, were injected subcutaneously into recipient mice. Two weeks later, a DTH response was measured to intrafootpad challenge with the eliciting peptide, and results were expressed as the increase in footpad weight of peptide-injected footpads over that of vehicle-injected (internal control) counterparts. The minority cell fraction was left untreated or treated for 24 h with NAS at 30 μM.

Real-time RT-PCR and Western blotting. Real-Time RT-PCR (for mouse *Ido1, Cyp1a1* and *Gapdh* and human *IDO1* and *ACTB*) analyses were carried out as described (2, 9, 10), using primers listed in Table S6. Data were calculated using the relative quantification method (ΔΔCT; means ± s.d. of triplicate determination), using *Gapdh* (for mouse cells) or *ACTB* (for human cells) as normalizer. Data are presented as normalized transcript expression in the samples relative to

normalized transcript expression in control cultures (in which fold change = 1; dotted line). Mouse IDO1 protein expression was investigated by immunoblot with a rabbit monoclonal anti-mouse IDO1 antibody (cv152)(11), whereas anti−β-tubulin was from Sigma-Aldrich. IDO1 expression in lysates of PBMCs was investigated by immunoblot with a mouse anti-human IDO1 antibody (clone 10.1; EMD Millipore Corporation). Anti−human β-tubulin antibody (Sigma-Aldrich) was used as a normalizer.

Measurements of IDO1 catalytic activity. L-kynurenine (Kyn) was measured by high performance liquid chromatography (HPLC) as described (12). Samples were kept frozen at −80 °C until analysis. The software TURBOCHROM NAVIGATOR 4 was used for evaluating the concentration of Kyn in samples by mean of a calibration curve. The detection limit of the analysis was 0.05 μM. For the analysis of the enzymatic activity of recombinant human IDO1 (rhIDO1; Giotto Biotech S.r.l.), NAS, dissolved in DMSO, was mixed in a final volume of 200 μl of a standard reaction mixture containing 50 mM potassium phosphate buffer (pH 6.5), 20 mM ascorbic acid (neutralized with NaOH), 200 μg/mL catalase, 10 μM methylene blue, 20 μM Trp, and 0.125 μg rhIDO1(12). The reaction was carried out at 37 °C for 60 min and stopped by the addition of 40 μl $HClO_4$ (Sigma-Aldrich). To complete the hydrolysis of N-formyl-kynurenine into Kyn, samples were heated at 65 °C for 15 min and then centrifuged at 12,000 rpm for 7 min at room temperature. The supernatant (200 μl) was transferred into a new Eppendorf tube and used for Kyn analysis.

Measurements of AhR activation. To assess the ability of NAS to activate AhR, we used mouse hepatoma (H1L1.1c2) cells, containing the stably integrated AhR xenobiotic responsive element driven by a firefly luciferase reporter plasmid, pGudLuc6.1 (13). Cells were seeded in 96-well plates at a density of 100×10^5 cells in 200 μl. After 12 h at 37 °C, cells were stimulated for 6 h with increasing concentrations of Kyn, as the reference AhR ligand, or NAS before lysis. Luciferase

assays were performed using luciferase reporter assay kit (Promega). The *Renilla* luciferase activity was measured, and results are presented as fold induction. In cDCs (1 x 10^6; purified from either WT or *Ido1*$^{-/-}$ mice), activation of Ahr was measured by RT-PCR (Table S6) in terms of increased expression of *Cyp1a1* transcripts induced by cell incubation with Kyn or NAS.

Docking Studies. The crystal structure of IDO1 containing IDE, cyanide and Trp (pdb code: 5WMV)(14) was downloaded from the Protein Data Bank (15). Chain A of the crystal structure was prepared for docking studies, removing water oxygens, cyanide and Trp, adding hydrogens and ionization states of charged residues at pH 7.0, with the *Protein Preparation Wizard* tool of *Maestro 10.1* (Maestro, version 10.1, Schrödinger, LLC, New York, NY, 2015; Schrödinger Suite 2015-1 Protein Preparation Wizard; LigPrep, version 3.3, Schrödinger, LLC, New York, NY, 2015; and Glide, version 6.6, Schrödinger, LLC, New York, NY, 2015). In order to remove potential steric clashes in the allosteric binding site, the resulting IDE-bound structure was energy refined using MacroModel Polak-Ribier conjugate method of energy minimization and the OPLS2005 force-field until a convergence gradient below 0.05 was successfully reached. Specifically, only atom residues within 12 Å from the centre of mass of IDE were considered as freely moving atoms, whereas remaining atoms were constrained on their atomic coordinates. A docking grid was next generated using *Glide* 6.6. The grid was centred on the centre of mass of IDE atoms. The inner grid box was sized 12x12x12 Å. The molecular structure of NAS was prepared for docking studies using *LigPrep 3.3*. Docking studies were carried out using *Glide 6.6* standard precision (SP) method. A two times enhanced sampling of ligand conformations and an expanded sampling of binding pose search were used for the docking procedure. The number of poses for the initial phase of docking was set to 50000, with a scoring window of 500 kcal/mol for keeping initial poses and the best 1000 poses kept for energy minimization.

After the docking procedure, the resulting binding poses of NAS (poses #1-#16, Table S2) were clustered using k-means algorithm applied on the root mean square deviation (RMSD)

calculated between the heavy atoms of each binding pose and the top energy scored binding pose (pose #1, Table S2), and visual inspection. As a result, a number of 8 clusters were found representing possible binding modes of NAS into the allosteric pocket of IDO1 (Fig. S5*A*-*G*). Cluster A contained the top energy scored binding pose (pose #1; Table S2) and was also the most populated including n.5 binding poses. Hence, the binding mode represented by cluster A with the top energy scored binding pose (pose #1) was selected for visual inspection and discussion of key interactions.

Genotyping and genetic association study. Genomic DNA was isolated from whole blood of MS patients and matched controls using the QIAcube automated system (Qiagen). SNPs spanning the *IDO1* gene were selected as described previously (10). Genotyping was performed using KASPar assays (LGC Genomics) in an Applied Biosystems 7500 Fast Real-Time PCR system (Thermo Fisher Scientific), according to the manufacturer's instructions. Quality control for the genotyping results was achieved with negative controls and randomly selected samples with known genotypes. In the genetic association study, the patients enrolled in the current study were analyzed in combination with a retrospective cohort previously described (PMID: 18208876). The association tests of *IDO1* alleles and genotypes with the risk of MS was performed using the Fisher's exact test. Multivariate analysis correcting for age of onset, gender, MS severity (according to EDSS values) and MS class (RRMS and PPMS) were based on conditional logistic regression analyses.

Statistical Analyses. All analyses were performed using Prism version 6.0 (GraphPad Software, Inc., La Jolla, CA). Data sets were first tested for normality using D-Agostino and Pearson omnibus normality test. The majority of data met normality and was analyzed by two-tailed unpaired Student's *t*-test. When data sets did not meet normality, the nonparametric Mann-Whitney test was used. All experiments were subject to at least three replicates per experimental parameter and overall results were shown as mean ± s.d. Association between two variables was analyzed by least

square regression analysis. EAE data were analyzed by 2-way ANOVA with two variables, time and treatment. To compare mean day of onset and maximal score, Mann-Whitney's rank-sum test was used (3, 16). All *n* values were computed by power analysis to yield a power of at least 80% with and alpha-level of 0.05.

References

1. E. Albini *et al.*, Distinct roles of immunoreceptor tyrosine-based motifs in immunosuppressive indoleamine 2,3-dioxygenase 1. *Journal of cellular and molecular medicine* **21**, 165-176 (2017).
2. M. T. Pallotta *et al.*, Indoleamine 2,3-dioxygenase is a signaling protein in long-term tolerance by dendritic cells. *Nat Immunol* **12**, 870-878 (2011).
3. F. Fallarino *et al.*, Metabotropic glutamate receptor-4 modulates adaptive immunity and restrains neuroinflammation. *Nature medicine* **16**, 897-902 (2010).
4. I. Mendel, N. Kerlero de Rosbo, A. Ben-Nun, A myelin oligodendrocyte glycoprotein peptide induces typical chronic experimental autoimmune encephalomyelitis in H-2b mice: fine specificity and T cell receptor V beta expression of encephalitogenic T cells. *European journal of immunology* **25**, 1951-1959 (1995).
5. C. Volpi *et al.*, Allosteric modulation of metabotropic glutamate receptor 4 activates IDO1-dependent, immunoregulatory signaling in dendritic cells. *Neuropharmacology* **102**, 59-71 (2016).
6. T. Liu, T. J. Chambers, Yellow fever virus encephalitis: properties of the brain-associated T-cell response during virus clearance in normal and gamma interferon-deficient mice and requirement for CD4+ lymphocytes. *J Virol* **75**, 2107-2118 (2001).
7. D. C. Fitzgerald *et al.*, Suppressive effect of IL-27 on encephalitogenic Th17 cells and the effector phase of experimental autoimmune encephalomyelitis. *J Immunol* **179**, 3268-3275 (2007).
8. U. Grohmann *et al.*, CTLA-4-Ig regulates tryptophan catabolism in vivo. *Nat Immunol* **3**, 1097-1101 (2002).
9. G. Mondanelli *et al.*, A Relay Pathway between Arginine and Tryptophan Metabolism Confers Immunosuppressive Properties on Dendritic Cells. *Immunity* **46**, 233-244 (2017).
10. C. Orabona *et al.*, Deficiency of immunoregulatory indoleamine 2,3-dioxygenase 1in juvenile diabetes. *JCI insight* **3** (2018).
11. L. Romani *et al.*, Defective tryptophan catabolism underlies inflammation in mouse chronic granulomatous disease. *Nature* **451**, 211-215 (2008).
12. E. Albini *et al.*, Identification of a 2-propanol analogue modulating the non-enzymatic function of indoleamine 2,3-dioxygenase 1. *Biochemical pharmacology* 10.1016/j.bcp.2018.10.033 (2018).
13. D. Han, S. R. Nagy, M. S. Denison, Comparison of recombinant cell bioassays for the detection of Ah receptor agonists. *BioFactors* **20**, 11-22 (2004).
14. H. C. Lewis, R. Chinnadurai, S. E. Bosinger, J. Galipeau, The IDO inhibitor 1-methyl tryptophan activates the aryl hydrocarbon receptor response in mesenchymal stromal cells. *Oncotarget* **8**, 91914-91927 (2017).
15. H. M. Berman *et al.*, The Protein Data Bank. *Nucleic acids research* **28**, 235-242 (2000).
16. K. K. Fleming *et al.*, Statistical analysis of data from studies on experimental autoimmune encephalomyelitis. *Journal of neuroimmunology* **170**, 71-84 (2005).